3*p* photoionization and subsequent Auger decay of atomic germanium

D. Anin,[1,*] K. Jänkälä,[1,2] S.-M. Huttula,[1] and M. Huttula[1]

[1]*Department of Physical Sciences, P.O. Box 3000, 90014 University of Oulu, Finland*

[2]*Institut für Experimentalphysik, Universität Hamburg, Luruper Chaussee 149, D-22761 Hamburg, Germany*

(Received 29 September 2012; published 17 December 2012)

The 3*p* photoionization and subsequent Auger decay of initially neutral atomic germanium is studied both experimentally and theoretically. The binding energies and relative intensities of the 3*p* photoelectron spectrum are given. The $M_{2,3}M_{3,4}M_{3,4}$ and $M_{2,3}M_{3,4}N$ Auger electron spectrum leading to doubly ionized final states is presented. The photoelectron and Auger electron spectra were interpreted using multiconfiguration Dirac-Fock calculations that provided the identification for the main spectral features.

DOI: 10.1103/PhysRevA.86.063410 PACS number(s): 32.80.Fb, 32.80.Hd

I. INTRODUCTION

Germanium and its compounds are important elements in modern electronics and especially in semiconductors. Since large amount of devices rely on germanium it is an attractive research subject. When germanium atoms bond, the outermost valence 4*s* and 4*p* orbitals hybridize and form delocalized bands. However, core orbitals remain localized in the solid germanium. Properties of these inner orbitals can be used as indicators of the chemical environment in the surface [1] and bulk [2], whereas the valence band provides information about the bonding itself [3]. Construction of solar cells with high efficiency and reliability is based on thin multilayer structures [4,5]. Thus the development of these structures requires tools sensitive to surface and chemical environment. A commonly employed method to probe the chemical environment is core-level photoionization and analysis of the chemical shift with respect to the atomic case. With synchrotron radiation it is possible to probe the properties of chemical bonds by studying the response of the system to photon impact and how it behaves in the subsequent Auger decay. During the past 50 years few studies of pure, doped mixed and solvated germanium [6,7] as well as germanium nanowires [8] were published. However, the basic knowledge of the electronic structure is not complete even for the atomic phase [9]. The present paper continues the effort on providing the basic electronic structure information about the core shells of industrially important metals (see, e.g. [9–11] and references therein). In the present paper experimental and theoretical analysis of the 3*p* ionization and subsequent Auger decay of atomic germanium is provided. The binding energies of the states related to Ge 3*p* photoionization and kinetic energies of the subsequent Auger decay are reported together with analysis and discussion of the observed spectral structures.

II. EXPERIMENT

The experimental work was carried out at the I411 beamline of MAX-II synchrotron storage ring in Lund, Sweden [12]. The electron spectra were measured using Scienta R4000 hemispherical electron energy analyzer. In order to obtain electron spectra that are proportional to the angle-integrated cross section, the electron signal were recorded at the angle of 54.7° with respect to the polarization vector of the synchrotron radiation. The evaporation of the germanium sample was performed using an inductively heated oven [13]. The sample was heated to ∼1500 °C in a graphite single-hole crucible. The 1 mm hole in the hat partially collimated vapor beam. Pass energy of 20 eV and 500 μm slit of the electron energy analyzer was used for the measurements and it corresponds approximately to the 100 meV contribution to the experimental broadening. The photon bandwidth for the chosen photon energies and beamline settings was estimated to be about 700 meV. In order to decrease noise caused by electromagnetic disturbances induced by the oven, measurements were vetoed during heating pulses. The binding and kinetic energies were calibrated with the aid of Xe 4*d* photoelectron lines and $N_{4,5}O_{2,3}O_{2,3}$ Auger electron lines, respectively [14]. The same lines were used for determining experimentally the analyzer transmission function using the constant ratio between the photoelectron and Auger spectral lines as discussed in Ref. [15].

The experimental spectra of both photoionization and Auger decay transitions were measured using three photon energies 175 eV, 185 eV, and 195 eV. The spectra are shown in Fig. 1. The photon energies were selected to be far away from the 3*p* binding energy to avoid postcollision interaction effect. The kinetic energy of the most intense Auger decay lines were found at 30–40 eV, and in addition smaller structure is seen at about 55–80 eV. In order to position the 3*p* photolines (with estimated binding energy at about 135 eV) out of the kinetic-energy region of the 3*p* and 3*d* Auger structures [16], photon energies above 250 eV would be needed. However, the need to avoid crossing the 3*s* ionization threshold at about 190 eV (see Ref. [17]) and the low ionization cross section of the 3*p* orbital over 100 eV above the ionization threshold prohibited the use of such high photon energies.

The three measured spectra, presented in Fig. 1, show the two main photoelectron line structures moving above the constant kinetic-energy Auger lines as the photon energy is varied. The spectra are normalized to each other by the Auger structures at 72–80 eV kinetic energy. A narrow line structure around 27 eV can be distinguished from the broad 3*p* related photoelectron and Auger signal. It consists of three lines at 27.2 eV, 27.5 eV, and 28.6 eV. Calculations predict the second step Auger decay transitions from $[\mathrm{Ar}]3d^8 4s^2 4p^2$ initial-state to $[\mathrm{Ar}]3d^9 4s^2$ final-state configuration to be at 27.1 eV and 27.6 eV kinetic energies, matching well to two of the narrow

*dmytro.anin@oulu.fi

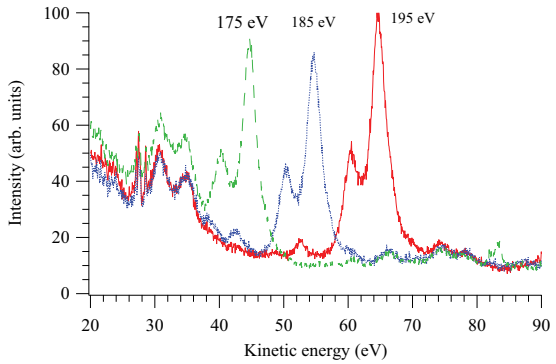

FIG. 1. (Color online) Experimental electron spectra of atomic germanium measured using incident photon energies of 175 eV (dashed green line), 185 eV (dotted blue line), and 195 eV (solid red line).

lines. However, the exact nature of the third narrow line is not known.

III. CALCULATIONS

The calculations for Ge $3p$ photoionization and Auger transitions were carried out with the multiconfiguration Dirac-Fock method. The atomic-state functions (ASFs) were obtained by diagonalizing the Hamiltonian matrix in the basis of jj-coupled antisymmetric configuration functions. The GRASP92 [18] package was used to solve the radial wave functions of the one-electron spin orbitals. The optimization of the radial wave functions was performed in the average level scheme where the orbitals were optimized by minimizing the average energy of the ASFs. The energies and mixing coefficient of atomic states were computed by utilizing the RELCI component of the RATIP package [19]. Further analysis of the states was done by changing the jj coupling to LSJ coupling using program LSJ [20].

The theoretical $3p$ photoelectron spectra of atomic germanium were obtained by calculating photon energy independent ionization probabilities using IONIS program [21]. The program assumes a constant ratio for the photoelectron partial waves and simply calculates relative transition probabilities. That has been shown to be a good approximation, if the photon energy is well above the ionization threshold [21].

According to the two-step model of the Auger process, the number of emitted Auger electrons e_A^- at the magic angle of 54.7° is proportional to the product of the total photoionization cross section and the relative Auger component rate. Including the photoionization of thermally populated initial states, the number of the emitted Auger electrons is given by

$$n_{f\beta} = \frac{2\pi \sum_{l_A, j_A} \left| \sum_{\mu\nu} c_{f\mu} c_{\beta\nu} M_{f\beta}^{\mu\nu}(J_f, J_\beta) \right|^2}{P_\beta(J_\beta)} Q_\beta(J_\beta), \quad (1)$$

where the $P_\beta(J_\beta)$ is the total decay rate and $Q_\beta(J_\beta)$ is the $|\Psi(J_i)\rangle \rightarrow |\Psi(J_\beta)\rangle$ ionization cross section. $M_{f\beta}^{\mu\nu} = \langle \Phi_\mu(J_f) \epsilon_A l_A j_A; J_\beta \| V \| \Phi_\nu(J_\beta) \rangle$ is the Coulomb matrix element. For more details about the AUGER program, see Refs. [9,19,22,23] and references therein.

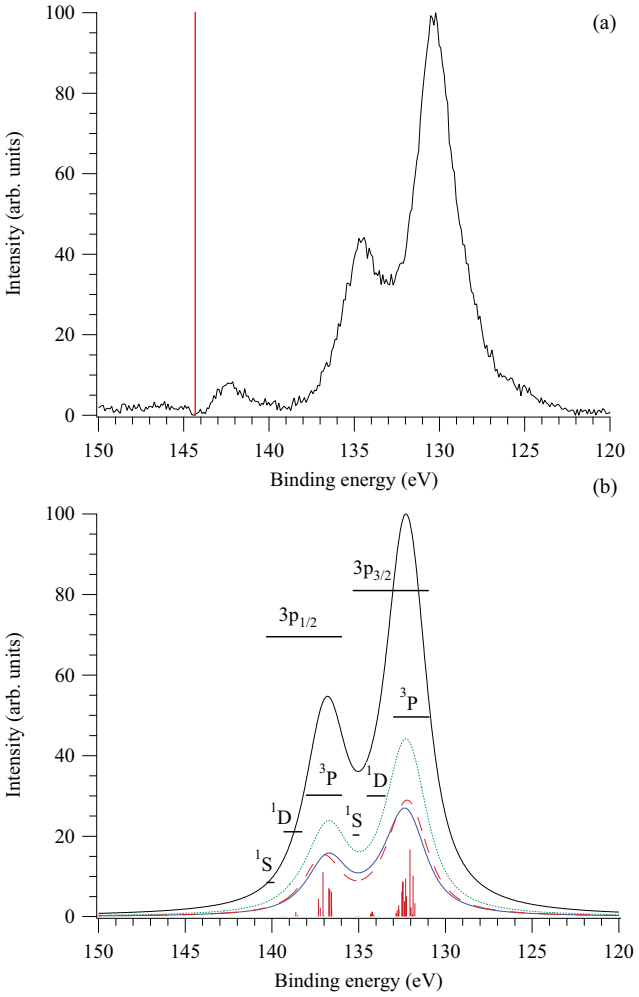

FIG. 2. (Color online) Experimental (a) and theoretical (b) photoelectron spectrum of atomic Ge. In the panel (a), to the right from the vertical bar is the experimental spectrum recorded at 195 eV photon energy and, to the left, the spectrum recorded at 175 eV photon energy. The uppermost solid line in the panel (b) is the overall predicted spectra. The three lines underneath, dotted (green), dashed (red), and solid (blue), are computed individual spectra of $^3P_1$, $^3P_0$, and $^3P_2$ initial states, respectively.

IV. RESULTS AND DISCUSSION

A. 3*p* photoelectron spectrum of atomic Ge

The experimental $3p$ photoelectron spectrum is shown in Fig. 2(a). It was obtained from the measured spectra shown in Fig. 1. To avoid the overlap of Auger lines the low binding-energy side from the vertical bar is formed by subtracting the Auger signal measured at 175 eV photon energy from the spectrum recorded at 195 eV photon energy.

The $3p$ photoelectron spectrum is dominated by two peaks located at binding energies of 130.3 eV and 134.7 eV. In addition, two satellite structures at 142.4 eV and 146.0 eV binding energy can be observed. The full width at half maximum of the main lines is about 2.6 eV. Since the experimental broadening is considerably smaller than the broadening caused by the lifetime, the line shape of the observed peaks is approximately given by the Lorentzian distribution. The binding energies and intensities of the features are listed in Table I.

TABLE I. Experimental and calculated binding energies (E_b) and relative intensities observed from 3p photoionization of atomic Ge. The energies are given in eV and intensities in arbitrary units.

Assignment	E_b Expt.	Intensity Expt.	E_b Theory	Intensity Theory
$3p_{3/2}$	134.65	100	132.34	100
^3P			132.25	95.16
^1D			134.23	4.71
^1S			135.05	0.13
$3p_{1/2}$	130.31	41.13	136.93	48.49
^3P			136.87	46.68
^1D			138.59	1.79
^1S			139.41	0.02
Satellites				
$3p_{3/2}$	142.35	8.44		
$3p_{1/2}$	146.03	1.18		

The photoelectron spectrum observed in Fig. 2(b) was modeled by single configuration [Ne]$3s^2 3p^{-1} 3d^{10} 4s^2 4p^2$ which gives 21 final states. The predicted lines were convoluted by 1-eV-wide Gaussian and 2.2-eV-wide Lorentzian profiles. The calculations gave Lorentzian widths of about 3.5 eV. These values are too high most likely due to overestimated Auger decay rates to low kinetic energies. Therefore, the experimentally observed Lorentzian width is used. The ground-state electronic configuration of atomic germanium [Ar]$3d^{10} 4s^2 4p^2$ consists of five fine-structure energy levels: $^3P_{0,1,2}$, $^1D_2$, and $^1S_0$. The energy separations between the ground state $^3P_0$ and the first two excited states $^3P_1$ and $^3P_2$ are 0.07 eV and 0.17 eV [24], respectively. Thus these levels are considerably thermally populated at the temperature used in the measurements. The third and fourth excited state, $^1D_2$ and $^1S_0$, are about 0.88 eV and 2.03 eV above the ground state [24] and have already negligible thermal population. The thermal populations for $^3P_{0,1,2}$ initial states, calculated from the Boltzmann distribution, are 0.277, 0.442, and 0.281, respectively.

In the 3p ionized configuration, coupling of the 3p hole to the two valence 4p electrons yields 21 fine structure states. Taking into account the population of the ground states, the simulated Ge 3p photoelectron spectrum is shown in Fig. 2(b). The three lines underneath the overall solid black line represent the individual spectra for the three lowest thermally populated states. Dashed (red) line, dotted (green) line, and solid (blue) line present the calculated spectra for $^3P_0$, $^3P_1$, and $^3P_2$ initially thermally populated states, respectively. The transition energies and intensities are presented as vertical bars in the figure. Comparing the prediction to the experiment we can identify the observed two structures arising from $3p_{3/2}$ and $3p_{1/2}$ spin-orbit split groups of lines.

In addition to the spin-orbit interaction of the 3p hole, the Coulomb interaction between the 4p valence electrons plays a role in the energy-level diagram of the 3p ionized states. Due to this, the $3p_{3/2}$ and $3p_{1/2}$ spin-orbit split lines are further separated into three groups that can be described by the intermediate LS coupling of the 4p electrons. The groups ^1S, ^1D, and ^3P are marked in Fig. 2(b). According to the calculations the mean energy separation of the groups is roughly the same as $^1S_0$, $^1D_2$, and $^3P_{0,1,2}$ initial states, which is reasonable since the Coulomb interaction between the 3p hole and the valence is quite small. Since 3p photoionization cannot directly change the coupling of the initially ^3P coupled valence electrons, the highest ionization cross section is observed for the $3p_j^{-1} 4p^2(^3P)_J$ final states. However, due to configuration interaction the calculations predict approximately 5% probability for ionization leading to low-spin $3p_j^{-1} 4p^2(^1D)_J$ and $3p_j^{-1} 4p^2(^1S)_J$ final ionic states as shown in Table I.

B. Auger decay

In the present experiments the photon energies used for excitation were chosen to show and separate three kinetic-energy regions. The spectrum measured at photon energy of 195 eV shows Auger structures at 25–50 eV kinetic energy without overlap of the photoline structures. The experiment performed at 175 eV photon energy gives the photoelectron signal including satellites below the main Auger structures at 25–50 eV kinetic energy, thus leaving the Auger signal at 50–80 eV kinetic energy range free of overlap. In addition, the spectrum measured at 185 eV photon energy provides Auger and photoelectron peaks identification cross-check in the low and high kinetic-energy tails. Figure 3(a) depicts the Auger electron spectrum combined from experiments recorded at 175 eV (right from the vertical line) and 195 eV (left from the vertical line) photon energies. The spectra are normalized to each other with the aid of the Auger signal at 72–80 eV kinetic-energy region. To remove the rapidly growing background towards low kinetic energies, power function approximation was used as a background in the fitting process.

The Auger electron spectrum following the 3p photoionization [Fig. 3(a)] presents spectral structures distributed to a more than 60-eV-wide kinetic-energy region. The most intense structure is found at 25–40 eV kinetic-energy region. The structure stems for Auger decay to [Ar]$3d^8 4s^2 4p^2$ final states. The considerably narrower lines at the left-hand shoulder of the structure at around 27 eV kinetic energy originate from second step Auger cascade transitions as described in Sec. II. In addition, a structure divided to five distinct smaller structures can be found at around 60–90 eV kinetic-energy region. This structure is due to overlapping Auger transitions to the [Ar]$3d^9 4s 4p^2$ and [Ar]$3d^9 4s^2 4p$ configurations.

The simulated 3p Auger spectrum is shown in Fig. 3(b). The predicted energy ranges and intensities of the spectrum are summarized in Table II together with the experimental values. As a general trend, the shape of the overall prediction

TABLE II. Experimental and calculated mean kinetic energies of 3p Auger decay lines of atomic Ge. The energies are given in eV and intensities in arbitrary units.

Assignment	Region Theory	Intensity Theory	Region Expt.	Intensity Expt.
$3d^8 4s^2 4p^2$	21.0–54.6	100.0	20.0–54.0	100.0
$3d^9 4s^2 4p$	68.4–89.8	12.4	70.9–90.0	31.4
$3d^9 4s 4p^2$	56.3–83.1	10.2	54.9–70.9	27.5
$3d^9 4p^3$	47.3–65.5	0.4		
$3d^{10}(4s^2, 4p^2)$	76.4–109.7	6.0		

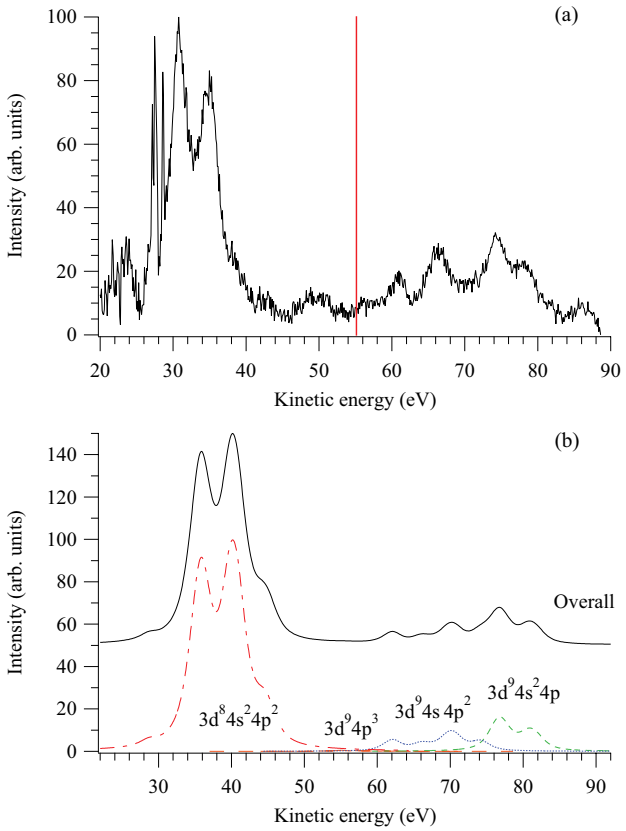

FIG. 3. (Color online) Experimental (a) and theoretical (b) electron spectra of the Auger decay following $3p$ photoionization in atomic germanium. In panel (a) to the right from the vertical bar is the experiment recorded at 175 eV photon energy and, to the left, is the spectrum recorded at 195 eV photon energy. In panel (b) the uppermost black solid line is the overall spectrum. The (red) dash-dotted depict the contribution for Auger decay to $3d^8 4s^2 4p^2$ configuration, (blue) dotted line for $3d^9 4s 4p^2$, and (green) dashed line $3d^9 4s^2 4p$ final-state configuration. In addition, position of the $3d^9 4p^3$ final electronic state is shown in the figure.

(solid black line) provides qualitative correspondence to the measurement. The final electronic configurations used in the calculations are $[\mathrm{Ar}]3d^8 4s^2 4p^2$, $[\mathrm{Ar}]3d^9(4s^2 4p, 4s 4p^2, 4p^3)$, and $[\mathrm{Ar}]3d^{10}(4s^2,\ 4p^2)$. The calculations predicted small Auger decay amplitudes to $[\mathrm{Ar}]3d^{10}(4s^2,\ 4p^2)$ final states at around 77–109 eV kinetic energy. However, no clear structures were seen in the kinetic-energy region at 90–109 eV in the experiment, where they should be visible without overlap with $[\mathrm{Ar}]3d^9 4s^2 4p$ structures. Auger decay leading to $[\mathrm{Ar}]3d^8 4s^2 4p^2$ final-state configuration is predicted to appear at 25–50 eV kinetic-energy region (red dash-dotted line), explaining the most intense double-peak–like structure with shoulderlike structure on its high kinetic-energy side. This decay channel gives about 80% of the total contribution to the total Auger decay rate, which is in agreement with the experiment. Due to heavy overlapping and wide natural linewidth it is impossible to assign any of the observed Auger peaks to single transitions. What can be said is that the highest Auger electron peak at about 30 eV kinetic energy can be assigned to arise from Auger decays of $3p_{3/2}$ initial states, whereas already the second highest peak at about 35 eV kinetic energy is a sum of transitions from both $3p_{3/2}$ and $3p_{1/2}$ initial-hole states to several Auger final states.

Calculated lines related to Auger decays leading to $[\mathrm{Ar}]3d^9 4s^2 4p$ and $[\mathrm{Ar}]3d^9 4s 4p^2$ final-state configurations are predicted to be found at 59–87 eV kinetic energy. The kinetic-energy region is well predicted as well as the number of the resolved structures. We may state that the two structures at around 61 eV and 66 eV center energies relate to Auger decays to $[\mathrm{Ar}]3d^9 4s 4p^2$ final electronic state configuration, while the high kinetic-energy features at center energies of 74 eV and 78 eV arise from decays to $[\mathrm{Ar}]3d^9 4s^2 4p$ final-state configuration. In addition, lines related to Auger decay to $[\mathrm{Ar}]3d^9 4p^3$ final-state configuration are predicted to be found at around 55 eV kinetic energy, possibly explaining the structure at about 50 eV kinetic energy. However, as the predicted intensity for this structure is very small and the photoelectron spectrum provided an overlapping satellite structure complicating the subtraction process, unambiguous assignment cannot be given.

V. CONCLUSIONS

In present work the $3p$ photoionization and the subsequent Auger decay of atomic germanium for initially neutral atoms have been studied experimentally and theoretically. The experimental spectra were analyzed using multiconfiguration Dirac-Fock calculations that provided fairly good agreement with the experiment. The binding energies of the $3p$ orbital and kinetic energies of the Auger decay following $3p$ ionization were provided together with analysis of the observed spectral features. The $3p$ photoionization is noted to reflect weak coupling of the valence shell electrons to the inner shell hole.

ACKNOWLEDGMENTS

This work has been financially supported by the Research Council for Natural Sciences and Engineering of the Academy of Finland and the European Community-Research Infrastructure Action under the FR6 "Structuring the European Research area" Programme (through the Integrated Infrastructure Initiative "Integrating Activity on Synchrotron and Free Electron Laser Science"). We thank the MAX-lab staff and Antti Kettunen for their assistance during the experiments.

[1] T. Weser, A. Bogen, B. Konrad, R. D. Schnell, C. A. Schug, and W. Steinmann, Phys. Rev. B **35**, 8184 (1987).
[2] D. Schmeisser, R. Schnell, A. Bogen, F. Himpsel, D. Rieger, G. Landgren, and J. Morar, Surf. Sci. **172**, 455 (1986).
[3] T. Barr, M. Mohsenian, and L. Chen, Appl. Surf. Sci. **51**, 71 (1991).
[4] R. R. King, D. C. Law, K. M. Edmondson, C. M. Fetzer, G. S. Kinsey, H. Yoon, R. A. Sherif, and N. H. Karam, Appl. Phys. Lett. **90**, 183516 (2007).
[5] M. Isomura, K. Nakahata, M. Shima, S. Taira, K. Wakisaka, M. Tanaka, and S. Kiyama, Sol. Energy Mater. Sol. Cells **74**, 519 (2002).

[6] J. M. Hunter, J. L. Fye, M. F. Jarrold, and J. E. Bower, Phys. Rev. Lett. **73**, 2063 (1994).
[7] J. R. Heath, Y. Liu, S. C. OBrien, Q. L. Zhang, R. F. Curl, F. K. Tittel, and R. E. Smalley, J. Chem. Phys. **83**, 5520 (1985).
[8] T. Hanrath and B. Korgel, J. Am. Chem. Soc. **126**, 15466 (2004).
[9] K. Jänkälä, R. Sankari, J. Schulz, M. Huttula, A. Caló, S. Heinäsmäki, S. Fritzsche, T. Rander, S. Svensson, S. Aksela, and H. Aksela, Phys. Rev. A **73**, 022720 (2006).
[10] L. Partanen, S. Fritzsche, K. Jänkälä, M. Huttula, S. Urpelainen, S. Osmekhin, H. Aksela, and S. Aksela, Phys. Rev. A **81**, 062513 (2010).
[11] K. Jänkälä, S. Urpelainen, M. Huttula, S. Fritzsche, S. Heinäsmäki, S. Aksela, and H. Aksela, Phys. Rev. A **77**, 062504 (2008).
[12] M. Bässler, A. Ausmees, M. Jurvansuu, R. Feifel, J. O. Forsell, P. de Tarso Fronseca, A. Kivimäki, S. Sundin, and S. L. Sorensen, Nucl. Instrum. Methods Phys. Res., Sect. A **469**, 382 (2001).
[13] M. Huttula, K. Jänkälä, A. Mäkinen, H. Aksela, and S. Aksela, New J. Phys. **10**, 013009 (2008).
[14] T. X. Carroll, J. D. Bozek, E. Kukk, V. Myrseth, L. J. Sthre, T. D. Thomas, and K. Wiesner, J. Electron Spectrosc. Relat. Phenom. **125**, 127 (2002).
[15] J. Jauhiainen, A. Ausmees, A. Kivimäki, S. J. Osborne, A. Naves de Briton, S. Aksela, S. Svensson, and H. Aksela, J. Electron Spectrosc. Relat. Phenom. **69**, 181 (1994).
[16] K. Jänkälä, D. Anin, S. Urpelainen, S.-M. Huttula, S. Heinäsmäki, and M. Huttula, Phys. Rev. A **84**, 052501 (2011).
[17] G. K. Wertheim and P. H. Citrin, in *Photoemission in Solids I: General Principles*, edited by M. Cardona and L. Ley (Springer-Verlag, Berlin, 1978), pp. 197–234.
[18] F. A. Parpia, C. F. Fischer, and I. P. Grant, Comput. Phys. Commun. **94**, 249 (1995).
[19] S. Fritzsche, J. Electron Spectrosc. Relat. Phenom. **114-116**, 1155 (2001).
[20] G. Gaigalasa, T. Zalandauskas, and S. Fritzsche, Comput. Phys. Commun. **157**, 239 (2004).
[21] S. Heinäsmäki, Comput. Phys. Commun. **183**, 431 (2011).
[22] S. Fritzsche, Comput. Phys. Commun. **183**, 1525 (2012).
[23] S. Fritzsche, J. Nikkinen, S.-M. Huttula, H. Aksela, M. Huttula, and S. Aksela, Phys. Rev. A **75**, 012501 (2007).
[24] National Institute of Standards and Technology (NIST), Atomic Spectra Database Energy Levels [http://physics.nist.gov/PhysRefData/ASD/].